

379  
N81d  
No. 802

MICROWAVE PROPERTIES OF LIQUIDS AND SOLIDS,  
USING A RESONANT MICROWAVE  
CAVITY AS A PROBE

DISSERTATION

Presented to the Graduate Council of the  
North Texas State University in Partial  
Fulfillment of the Requirements

For the Degree of

DOCTOR OF PHILOSOPHY

By

Ki H. Hong, B. S., M. S.

Denton, Texas

May, 1974

Hong, Ki H., Microwave Properties of Liquids and Solids, Using a Resonant Microwave Cavity as a Probe. Doctor of Philosophy (Physics), May, 1974, 66 pp., 4 tables, bibliography, 27 titles.

The frequency shifts and Q changes of a resonant microwave cavity were utilized as a basis for determining microwave properties of solids and liquids. The method employed consisted of varying the depth of penetration of a cylindrical sample of the material into a cavity operating in the  $TM_{010}$  Mode. The liquid samples were contained in a thin-walled quartz tube. The perturbation of the cavity was achieved by advancing the sample into the cavity along the symmetry axis by employing a micrometer drive appropriately calibrated for depth of penetration of the sample. A differentiation method was used to obtain the half-power points of the cavity resonance profile at each depth of penetration. The perturbation techniques for resonant cavities were used to reduce the experimental data obtained to physical parameters for the samples. The probing frequency employed was near 9 GHz.

TABLE OF CONTENTS

	Page
LIST OF TABLES . . . . .	v
LIST OF ILLUSTRATIONS . . . . .	vi
Chapter	
I. INTRODUCTION . . . . .	1
II. EQUIPMENT DESIGN AND CONSTRUCTION . . . . .	7
III. EXPERIMENTAL RESULTS AND CONCLUSIONS . . . . .	40
Appendices	
I. PHYSICAL DIMENSION OF SAMPLES . . . . .	56
II. CHECK TO DETERMINE THE ADDITIVE PROPERTY OF THE RESONANT FREQUENCY SHIFTS USING TWO DIFFERENT RADII QUARTZ TUBES . . . . .	57
III. EXPERIMENTAL DATA FOR SOLIDS STUDIED . . . . .	69
REFERENCES . . . . .	62
BIBLIOGRAPHY . . . . .	64

## LIST OF TABLES

Table	Page
I. Data Used for Linearity Check of Tuned Amplifier for Each Gain Setting . . . . .	22
II. Experimental Values of Microwave Parameters for Liquids and Solids. . . . .	50
A-I. Physical Dimension of Samples. . . . .	56
A-III. Experimental Data for Solids Studied . . . . .	61

## LIST OF ILLUSTRATIONS

Figure	Page
2-1. Frequency Multiplication Processes. . . . .	10
2-2. Observed Microwave Signals. . . . .	15
2-3. Chopper Wave Modulated Signal . . . . .	16
2-4. Resonance Absorption and Cavity Perturbation Signals . . . . .	17
2-5. Output Potential vs. Microwave Power Input Using Tuned Amplifier. . . . .	23
2-6. Calibration Curve for Narda Model 810 Wavemeter Calibrated to General Radio Standard 1112A and 1112B . . . . .	26
2-7. Various Types of Tuned Circuits . . . . .	28
2-8. Microwave Cavity Geometry . . . . .	32
2-9. Electromagnetic Field Intensity and Field Distortion Around the Iris Holes . . . . .	33
2-10. Sample Probing into Microwave Cavity. . . . .	36
2-11. Experimental Arrangement. . . . .	38
3-1. Behavior of Resonant Frequency Shift vs. Various Amounts of Benzene Admitted into the Resonant Cavity Along Its Symmetry Axis. . . . .	44
3-2. Resonant Frequency Shifts vs. Various Liquid Sample Volumes After Iris Effect Has Been Removed from the Experimental Data. . . . .	47
3-3. Experimental Data for $\Delta w$ vs. $\Delta f$ to Deduce Loss Tangents. . . . .	52
A-1. Check for Additive Property of the Resonant Frequency Shifts Using Two Different Radii Quartz Tube. . . . .	59

## CHAPTER I

### INTRODUCTION

Measurements of dielectric constants, either in static or time varying field, are important in studying the electrical characteristics of material properties. In order to make studies of material properties, resonant circuit methods have been widely employed in experimental apparatus. Some restrictions are imposed upon the experimental apparatus in the measurement of electrical properties of materials, depending upon the various frequency regions being explored. In the region of frequency up to  $10^7$  Hz, a Schering bridge can be used for studies of the dielectric properties<sup>1</sup>. Resonant circuit methods are employed in the frequency region of  $10^4$  Hz -  $10^8$  Hz.

At frequencies above  $10^8$  Hz, lumped resonant circuit methods are not proper devices because of the large unaccountable energy losses into the space around the circuits.

In this frequency region ( $10^8$  Hz and higher), waveguide elements are required to operate the experiment properly. The basic difference between the lumped circuit and the microwave resonant cavity is that the current and voltage are replaced by electromagnetic fields. The microwave resonant cavity displays the same resonant characteristic as a tuned

circuit. Either in the lumped resonant circuits or the resonant cavity, the quality factor  $Q$  is determined from the resonant curve shape.

The  $Q$  factor is defined as the ratio of the resonant center frequency to the half-power frequency width of the resonant curve. It is very hard to obtain a  $Q$  of several hundred in the simple tuned LC circuit, but  $Q$  of several thousand can be easily obtained in the resonant cavity, because of low resistances. The measurement of dielectric properties of materials at microwave frequencies can be made by the microwave cavity method.

The microwave technique is not a new method but a standard technique employed if one wants to investigate dielectric or plasma properties<sup>2</sup>. By placing the material into localized microwave electric or magnetic fields in the cavity, either electric permittivity or magnetic permeability can be determined. The method can be applied to plasma experiments by placing the plasma in the cavity and determining electron density from a measurement of resonant frequency shift<sup>3</sup>. One cavity perturbation theory was introduced by Bethe and Schwinger<sup>4</sup> in 1943, and another by Slater<sup>5</sup> in 1946. According to the Bethe-Schwinger perturbation theory, the fields of the cavity should be altered in form only slightly from the original configuration of the empty cavity, upon the insertion of the sample. This does not necessarily mean that the change in the stored energy of the cavity be small upon

introduction of the sample into the cavity. The electromagnetic energy can be pumped into the cavity, and the stored energy can be kept constant.

According to Slater's perturbation theory, the introduction of a sample into the cavity causes the resonant frequency shift and the cavity Q change to occur. Simple and useful expressions were derived for interaction of electromagnetic fields and material properties. The perturbation theory, introduced either by Bethe-Schwinger or Slater, is basically the same. One of the results from these theories is that if the cavity wall is pushed in by a small amount, the electromagnetic fields in the cavity are disturbed, and the perturbation causes the resonant frequency of the cavity to be raised. Essentially, the resonant frequency shift and the cavity Q change due to the insertion of the sample show the characteristic electrical properties of the material, and it is known that the resonant frequency shift and the cavity Q change are usually proportional to the perturbation volume within the region of validity of the perturbation theory.

The perturbation of the resonant microwave cavity has been utilized to determine the dielectric property of liquids, gases, and plasma in a tubular container or solid cylinder. The perturbation theory was derived based on the fact that the electromagnetic field wavelength in the cavity (cavity volume) was assumed to be very large compared to the sample dimension.



In this experiment the approximate ratio of the volume of the sample to the volume of the cavity was made variable by using a mechanical drive to advance the sample into the cavity. In this experimental operation, the rod-shaped sample diameter is very small compared with the wavelength of the cavity field, so that the external applied field is assumed to be uniform over the region in which the sample is inserted. The rod is placed at a position of zero magnetic field (maximum electric field), so that magnetic effects can be considered to be negligible. Using the perturbation method, dielectric constants can be determined from the resonant frequency shift of the cavity with and without the sample.

The resonance method of dielectric measurement at microwave frequencies, using cylindrical cavities partially filled with a solid dielectric rod was worked out by Hornel and his collaborators<sup>6</sup>. In 1952, Maier and Slater<sup>7</sup> introduced metallic conducting sphere, disk and needles of different diameter into a cavity and employed the perturbation method to compare their experimental measurements with theoretical results.

Furthermore, some measurements of the dielectric constant at microwave frequencies were reported by Bhar<sup>8</sup>, 1963; Gerdes, et al.<sup>9</sup>, 1969; Srivastava, et al.<sup>10</sup>, 1971. In 1956, a similar experiment for a sphere of magnetic material was worked out by Spencer, Le Crow and Ault<sup>11</sup>. A year later, Tompkins and Spencer<sup>12</sup> reported retardation effects on a magnetic sphere and a rod using Bethe-Schwinger perturbation

theory. They also presented frequency shifts of a cylindrical cavity ( $TM_{110}$  mode) caused by a thin cylindrical rod placed along the cavity axis.

In 1962, Kaminow and Harding<sup>13</sup> measured the temperature dependence of the complex dielectric constant of  $KH_2PO_4$  at the resonant frequency of 9.2 GHz using a cavity perturbation method. In 1964, exact evaluation of the dielectric constant of a pyrex tube at the resonant frequency of 3 kHz was worked out by Sen, Basu and Ghoshal<sup>14</sup>, and they also compared the experimental and theoretical dielectric constant for pyrex.

Recently, an exact solution and perturbation results for frequency shift and Q deterioration of  $TE_{011}$  cylindrical cavity by coaxial loading with a scalar dielectric were reported by Haniotis and Gunthard<sup>15</sup>. Also, the frequency shift and the cavity Q change of a microwave cavity caused by lossy dielectrics and plasmas in spherical or cylindrical boundaries were calculated by Hall<sup>16</sup>. His discussion concerned what range of values of permittivity, conductivity and radius of metallic sphere or rod for a perturbing volume could produce frequency shifts. At present, it is obvious that the microwave techniques are standard and common practice in studying electric properties of materials.

In this investigation, dielectric constants were to be obtained from relative frequency shifts and the cavity Q changes for various volumes. Liquids and solids were studied

in order to determine the relationship between material volume and frequency and Q change. Partially inserted in the cavity, the materials interact with the electromagnetic fields in the cavity and produce a perturbation which causes the field configuration to change. The field redistribution in the cavity causes the resonant frequency of the cavity and the Q factor to change.

The experimental measurement of the resonant frequency shift and the cavity Q change in the cylindrical cavity, which was operated in  $TM_{010}$  mode, for the volume change of solids and liquids coaxially placed in the probing cavity enabled the characteristic properties of materials to be obtained. Various samples were introduced into the cavity and the resulting perturbation effects on the resonant frequency shifts and the cavity Q changes were studied.

In general, dielectric properties are temperature and frequency dependent. The experiment was performed keeping the cavity at room temperature.

Chapter II deals with instrumentations. Properly interpreted, the experimental results yield the microwave properties of materials and are treated in Chapter III.

## CHAPTER II

### EQUIPMENT DESIGN AND CONSTRUCTION

In this chapter a discussion is given of each part of the equipment which was unique to this experimental investigation. Since the investigation relied upon a complete knowledge of the shape and the width of the resonance profile associated with a cylindrical cavity operating in the  $TM_{010}$  mode, it is necessary to fully understand the instrumentation utilized in deriving these resonance parameters.

#### Reflex Klystron

The source of electromagnetic radiation of millimeter or centimeter wavelength can be usually obtained from an electronic tube, which is called a reflex klystron. The reflex klystron is a device that generates a microwave oscillating electromagnetic field whose frequency primarily depends on the physical size of a cavity resonator. Basically, the reflex klystron utilizes a single resonator for electron bunching and catching which arises from different transit time of electrons, and develops feedback by reflecting the electron beam so that it passes through the resonator a second time.

Specific details of the klystron operation will not be discussed in this paper since basic operations of the klystron are described in standard microwave electronic<sup>17</sup>. The V-58 type klystron was used for this experimental operation.

#### Frequency Multiplier

Interpolation of the frequency markers is achieved by means of a radio receiver. In order for the radio receiver to work, the intermediate frequency should be swept through in the mixing process. In order to meet the mixing requirement, another source of high order frequency comparable to the klystron resonant frequency must be supplied to the crystal detector which is in the directional coupler. Such high order frequencies, for the mixing process, can be obtained from a frequency multiplier.

The frequency multipliers used for the frequency measurement were the model 900B Sweep Signal Generator by Jerrold Electronics, Corporation and models 1112A and 1112B General Radio Standards. The former type of the frequency multiplier has two band selections and covers a frequency range up to 1 KMHz.

In the frequency multiplication process, the generation of an output signal is synchronized with the input and a component of the desired output frequency. Normally, the desired output associates with both desired and undesired components. By using a band pass filter the desired

frequency component can be selected. The important thing is that harmonic generation of frequency multipliers requires a high degree of non-linearity in the multiplying element, which is usually a crystal diode. The basic accuracy of the standard frequency system is determined by a Hewlett-Packard model 524-D electronic counter. A crystal oscillator is arranged in the frequency multiplier to produce initial harmonics of relatively low frequencies. The initial r-f signal is generated in a crystal oscillator at 5 MHz.

The subsequent frequency standard devices are set to multiply the initial standard frequency. The initial standard frequency utilizes a chain of frequency multiplication through r-f amplifiers and multipliers. Thus, the high order frequency output can be available for the mixing process. The crystal mixer rectifies the r-f signal and the rectified wave is known to be the resultant of components of harmonic wave. Fourier analysis of the non-sinusoidal periodic wave form shows the rectified wave is made of sinusoidal components whose frequencies are integral multiples of the fundamental frequency of the non-sinusoidal periodic wave form. When a sine wave input is applied to a circuit that has non-linear transfer characteristics, the output is non-sinusoidal and contains synchronized harmonics of the fundamental sine wave. The electronic details will not be discussed in this section. Instead, the multiplication process can be understood by referring to the

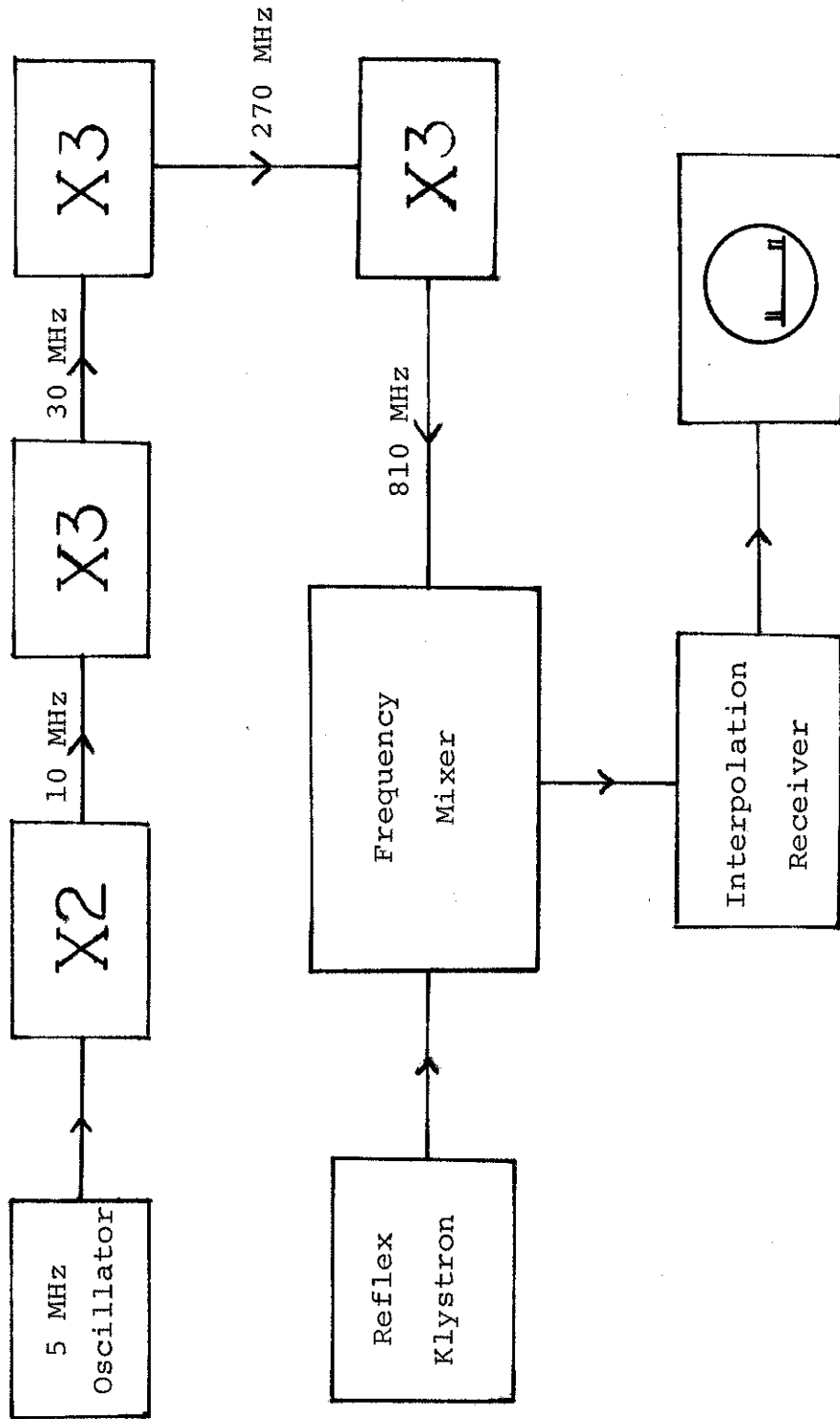


Fig. (2-1) Frequency multiplication processes

schematic diagram shown in Fig. (2-1). The initial frequency 5 MHz in the crystal oscillator is doubled to 10 MHz through push-push doubler circuits. The resulting 10 MHz drives a push-pull tripler circuit using a standard multiplying device. Through this procedure, 30MHz is obtained. The multiplication is continued by repeating the above procedure until finally a high-order harmonic output is delivered into the mixer.

Fig. (2-1) shows the multiplication processes whose initial 5 MHz harmonic waves are increased up to 810 MHz.

The output high-order frequencies are delivered to the crystal detector and the mixing process occurs. Since the arbitrary  $n^{\text{th}}$  harmonic wave from the frequency multiplier can be matched to the modulated klystron frequency, the frequency difference can be received by the radio receiver. When the General Radio model 1112A and 1112B standards are employed the same technique is used and only the fundamental frequencies are changed.

#### Frequency Marker Detection and Display

The interpolation method was used for frequency marker intervals and frequency reference. Definite frequency marker references (both intervals and absolute) were essential when resonant frequency shift and cavity Q change are required to be measured. The method was to zero beat two frequencies, one from the klystron and one from a frequency standard, which produced two reference frequency markers.



The radio receiver used for the interpolation method was a model B.C.-348-Q made by Wells Cardner & Company. Use of the radio receiver permits the frequency standard, when heterodyned with the klystron frequency, to generate low frequency intervals. When the klystron signal is heterodyned against the standard frequency source and monitored by the interpolation receiver, its position on the frequency scale is located by marker "beats" whose separation can be read. Thus, the radio receiver can be used for the frequency reference markers and at the same time for absolute frequency measurement.

The modulated klystron microwave signal is transmitted through the main waveguide that is coupled to a directional coupler. The crystal mixer installed in the coupler receives this microwave signal. On the other hand, the low order harmonic frequencies originating from the crystal oscillator in the frequency multiplier are increased to high order harmonic in the same diode through the multiplication process.

The final output harmonic waves occur in the crystal mixer where the mixing processes can be achieved. The radio receiver responds to only the frequency difference between the klystron resonant frequency and an  $n^{\text{th}}$  harmonic wave frequency multiplier. If the interpolation receiver is adjusted to a certain frequency band, the radio receiver detects the mixing frequency difference mentioned above.

The resulting frequency difference yields two frequency markers which are displayed on the oscilloscope and the recorder traces to be used as frequency reference markers. The appearance of the markers is the frequency difference separation given by the following equation,

$$f_r = f_s \pm n f_m \quad (2-1)$$

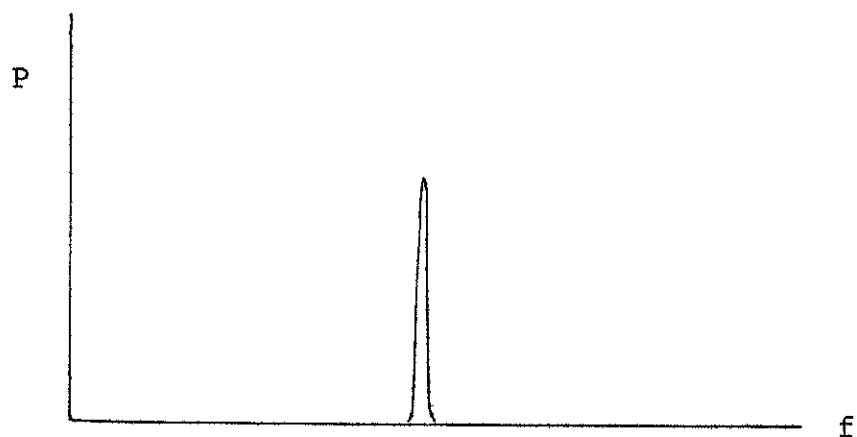
where  $f_r$  is the frequency to which the radio receiver is tuned,  $f_s$  is the modulated klystron frequency,  $f_m$  is the frequency from the frequency multiplier, and  $n$  is the order of harmonics. The plus or minus sign which appears in Eq. (2-1) indicates that the local oscillator signal can mix from either a sum or difference with the center frequency of the klystron. The marker appearance depends on the wave form, frequency and amplitude of the klystron modulation. In this operation, the frequency region used for the reference markers lies between zero and 36 MHz. The width of the band can be widely selected by the radio receiver. The type B.C.-348-Q radio receiver has a variety of frequency bands that ranges from 400 kHz to 36 MHz. The absolute frequency measurements were determined by a General Radio Model 1112A and 1112B set of harmonic generators properly stabilized. A wavemeter was also used to measure coarse frequencies.

## Signal Shape and Modulation

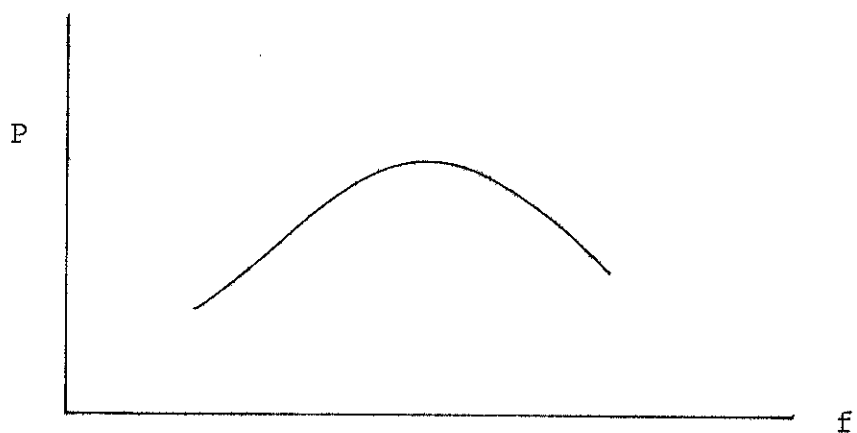
### Signal Shape

The reflex klystron generates electromagnetic waves and the electromagnetic energy is transmitted through a waveguide to the cavity. As shown in Fig. (2-2-i), the microwave power generated from the reflex klystron gives only a narrow frequency interval; the horizontal axis is frequency and the vertical axis is microwave power. Modulating the signal with the oscilloscope horizontal sawtooth sweep voltage that is synchronized with the klystron repeller, the klystron "mode" appears as shown in Fig. (2-2-ii). The placement of the cavity at the end of the waveguide permits the part of microwave power to be reflected and the reflected microwave power can be detected by a suitable diode. As shown in Fig. (2-2-iii), the dip represents the cavity resonance absorption displayed in an oscilloscope by observing the microwave radiation signal reflected from the cavity. The power absorption dip indicated in the dotted circle as shown in Fig. (2-2-iii) is the major interest in studying microwave interaction with the dielectrics.

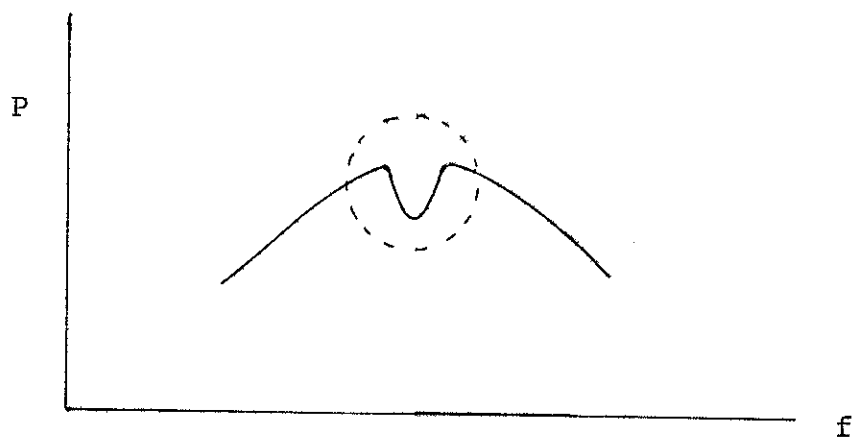
As the sample is inserted into the cavity, the sample perturbs the electromagnetic field in the cavity. Consequently, the resonant frequency shifts and the cavity Q changes. According to Slater's perturbation theory<sup>5</sup> the resonant frequency shifts and the cavity Q changes are



(i) Klystron mode shape (natural width)



(ii) Klystron mode shape modulated by an oscilloscope horizontal sawtooth sweep.



(iii) Reflected power absorption by cavity

Fig. (2-2) Observed Microwave Signals

functions of the dielectric property and its perturbation change. In the experimental operation, these resonant frequency shifts and the cavity  $Q$  changes can be observed in the following way. The power absorption is reflected by the cavity and the signal can be detected by a suitable crystal rectifier. As the sample is incrementally placed into the cavity, the position of the power absorption, i. e., the resonant frequency, is observed to be shifted and the absorption shape is distorted. Since the signal made by the cavity power absorption was not strong enough, a tuned amplifier was employed to amplify the signal. One is generally interested in the resonant shape of the power spread within the dotted circle as shown in Fig. (2-2-iii) and the enlarged dotted circle has been redrawn in Fig. (2-3-i).

Through the r-f amplifier, the final form of the sine wave modulated reflected signal can be obtained as shown in Fig. (2-3-ii).

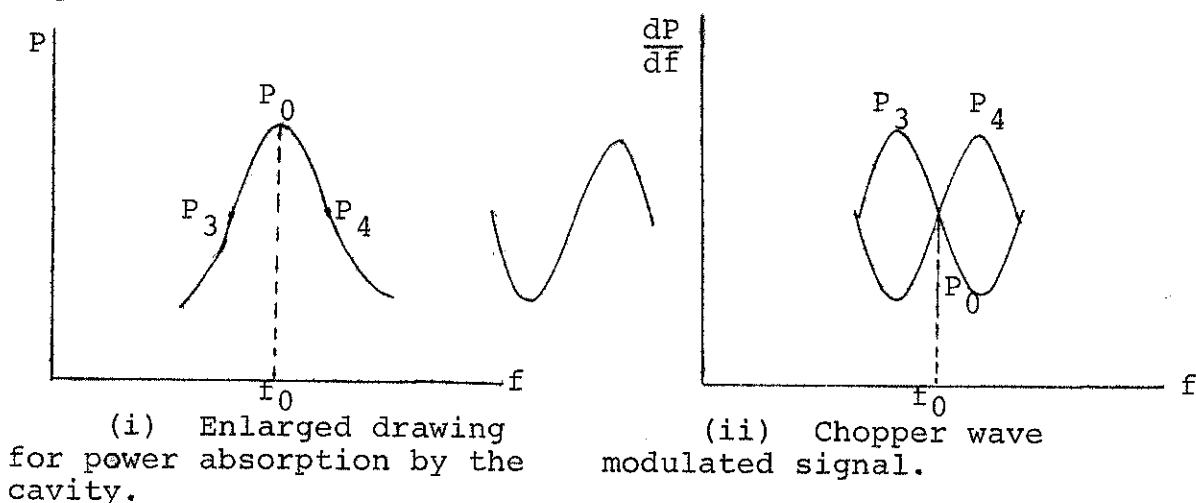


Fig. (2-3) Chopper wave modulated signal

In order to simplify the measurement, the absorbed signal due to the unloaded cavity can be conveniently modulated by applying a "chopper" wave voltage to the repeller electrode of the reflex klystron and, thus, a differentiated display of the resonance profile can be obtained. The differentiated signal is more convenient to measure the unknown frequency spacings and is more accurate since it is not generally easy to determine the half power frequency width directly from observed resonant absorption shape. If the signal is differentiated, the frequency interval measurement will be a measurement between  $P_3$  and  $P_4$  for the cavity  $Q$  change, and the measurement of  $P_0$  will give the resonant frequency shifts as shown in Fig. (2-3-ii). Fig. (2-4) shows relative cavity  $Q$  change and the resonant frequency shifts. The points  $P_3$  and  $P_4$  must be related to the half power points as discussed

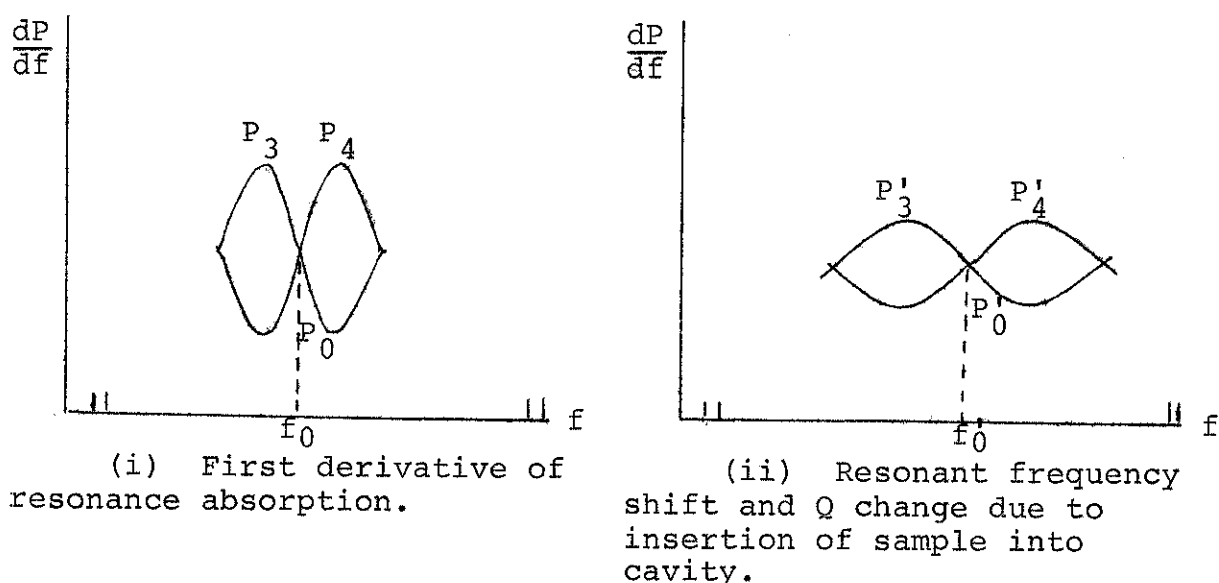


Fig. (2-4) Resonance absorption and cavity perturbation signals.

in the next section. These resonant frequency shifts and the cavity Q change are produced by the sample insertion into the cavity.

### Modulation

The microwave source (reflex klystron) requires modulation in order to derive a time varying signal since the unmodulated source gives only a single frequency. It is desired that the signal is not distorted any more than necessary.

The modulation voltages for the klystron are provided from two sources.

- (1) The oscilloscope horizontal output wave form was coupled to the klystron repeller electrode and provided the sawtooth sweep voltage. Providing sawtooth sweep voltage to the klystron gives signals as shown in Fig. (2-2-ii).
- (2) The high frequency sine wave voltage was applied to the repeller of the klystron to "chop" the signal.

Application of sine wave voltage to the reflex klystron caused the signal to be differentiated as shown in Fig. (2-3-ii). The modulation signal for this purpose was derived from a signal generator model EUW-27 made by Heath Company. The sine wave frequency of this unit lies between 20 Hz and 1 MHz. In order to obtain the first differentiation for the signal, the modulator frequency employed was 42 kHz as this was the

resonant frequency of the tuned amplifier. For the higher order differentiation, the klystron frequency was modulated sinusoidally with a frequency of  $42/n$  kHz where  $n$  is an integral number and in the range 1 to 5. The modulated signal shape arising by application of a sine wave voltage was studied by Roberts, et al<sup>18</sup>.

The correction equation for frequency measurement in which  $n$  is 1 when applying the sine wave modulation is given by<sup>19</sup>

$$2\delta v = \frac{2}{\sqrt{3}} \Delta v \left[ 1 + \frac{1}{4} \left( \frac{\omega'}{\Delta v} \right)^2 + \left( \frac{f}{\Delta v} \right)^2 \right] \quad (2-2)$$

where  $\Delta v$  is the half width,  $\omega'$  is the frequency deviation of the klystron modulation or the marker pair separation, and  $f$  is the modulation frequency. In the experimental operation, it was observed that the frequency of modulation and the marker pair spread due to the modulation are negligible compared with the half-width frequency.

#### Detector Response and Amplification

Another vital device in this operation was a detector which is used for the r-f wave. The detector is an element, usually semiconductor crystal which produced demodulation of an r-f wave. Usually, semiconductor crystals are used for detection of microwave power. The crystal detector consists of a fine wire in contact with a block of semiconducting



material. The contact resistance in one direction is higher than in the reverse. The current-voltage characteristic is very non-linear and rectification can be made when an alternating voltage is applied. Since the detector has fine contact point, the rectifier can be used to extremely high frequencies. The sensitivity of a crystal is determined by the ratio of its forward to a reversed current impedences. To detect the signal, a 1N23F crystal detector was used to take power from the waveguide. The crystal detector usually produces an output current such that the current-voltage characteristic is represented by  $I \propto V^2$ . The output power is approximately proportional to the square of the input power, that is

$$P_{\text{out}} \propto I^2 \propto V^4 \propto P_{\text{in}}^2. \quad (2-3)$$

For small change of the input power, Eq. (3-3) yields

$$\Delta P_{\text{out}} \propto P_{\text{in}} \Delta P_{\text{in}}. \quad (2-4)$$

The characteristics of the detector must be well understood when resonance shape studies are made. A small power input to the cavity produces absorption due to field interacting with the dielectric in the cavity and gives a relatively large change in output signal. The power adjustment must be made such that the distortion is insignificant. Another important usage made of crystal detectors is in the harmonic generation. Since the rectified signal is the resultant component of all harmonic waves, the crystal detector can be

well used as a superheterodyne mixer, especially at microwave frequencies. In this experimental operation, a crystal detector was installed in the reflectometer to provide dc output when modulated microwaves are reflected from the resonant cavity. Another 1N23 crystal detector was mounted in a directional coupler to mix the modulated klystron signal with the  $n^{\text{th}}$  harmonic waves from the frequency multiplier, (standard frequency generator).

#### Tuned Amplifier

The observed signal is not well enough defined to make accurate measurements of the cavity  $Q$  change directly. A tuned amplifier was used to produce clearly defined signals for accurate frequency measurement and to reject unwanted noise which might be near the resonances being observed. The tuned amplifier was checked for several different gains with linearity check made for various input and output voltage as shown in Fig. (2-5) and Table I. The signal displayed on the oscilloscope through the tuned amplifier was observed whether it was distorted or not. Distortion was kept minimized over the signal ranges observed.

#### Waveguide System

The waveguide system used in this laboratory consists of main waveguide, directional coupler, reflectometer, variable attenuator, wavemeter and cylindrical cavity. All of these

TABLE I  
 DATA USED FOR LINEARITY CHECK OF TUNED  
 AMPLIFIER FOR EACH GAIN SETTING

Output in Volts	Input in Volts for Each Gain Setting					
	1	2	3	4	5	6
0.1	0.0065	0.0028	0.002	0.0015	0.0012	0.001
0.2	0.0013	0.0054	0.004	0.003	0.0026	0.002
0.3	0.019	0.0082	0.0058	0.0045	0.0038	0.0031
0.4	0.026	0.0110	0.0080	0.0062	0.0049	0.0040
0.5		0.0140	0.0102	0.0074	0.0062	0.0052
0.6		0.017	0.012	0.0090	0.0074	0.006
0.7		0.0194	0.014	0.0104	0.0087	0.0070
0.8		0.022	0.016	0.0120	0.0100	0.0080
0.9		0.025	0.018	0.0134	0.011	0.0090
1.0			0.02	0.0150	0.0124	0.010

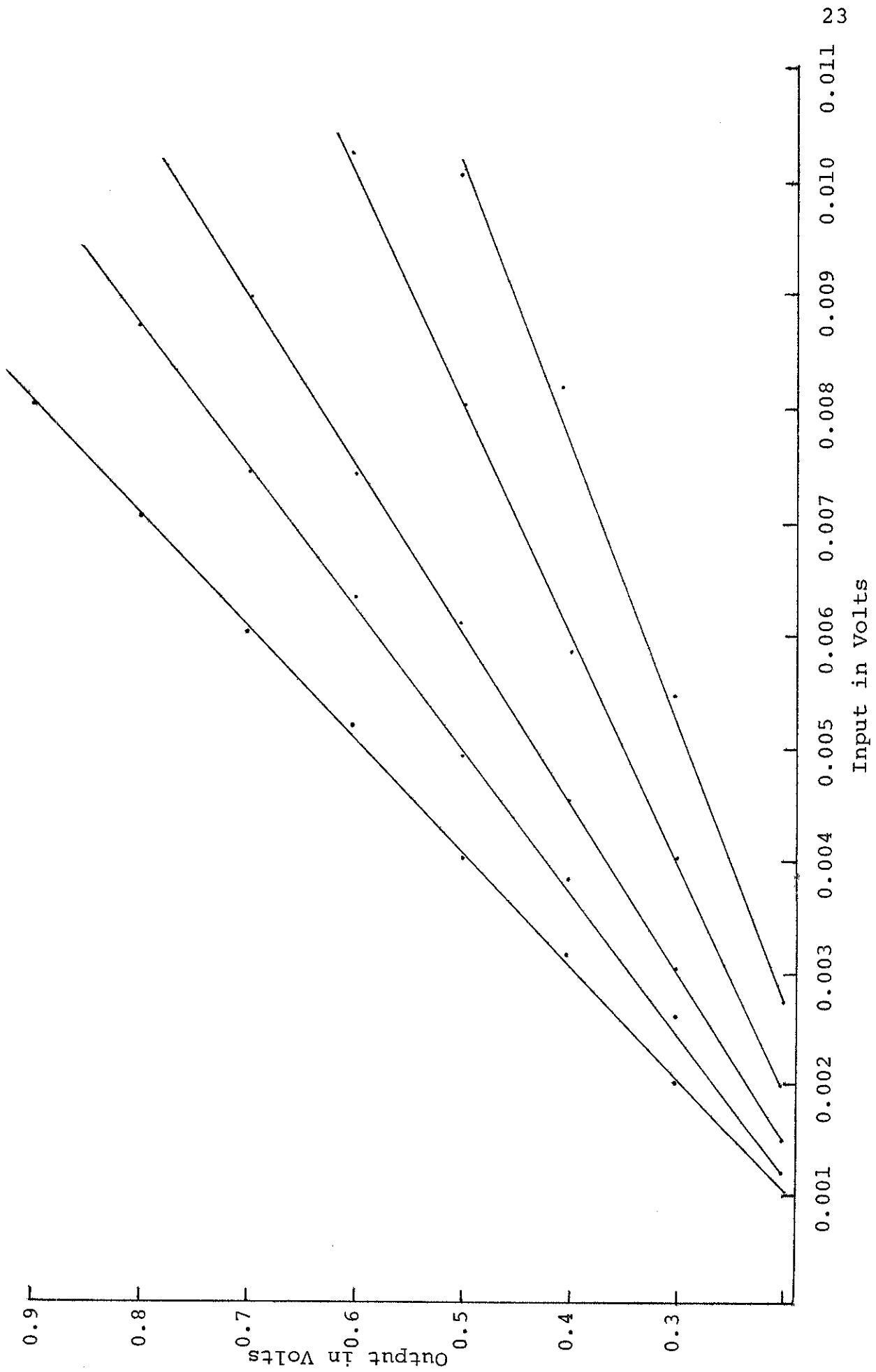


Fig. (2-5) Output potential vs. microwave power input using tuned amplifier

are commercial units except the sample probing cavity. The main waveguide is a device made of a hollow conductor through which electromagnetic waves propagate. The directional coupler contains a 1N23 crystal diode in which the resonant frequency of the reflex klystron and the  $n^{\text{th}}$  harmonics of the frequency multiplier are mixed together to obtain the frequency marker system. The reflectometer also contains another 1N23 crystal diode which can be used for the detection of the reflected signal from the cylindrical cavity. The variable attenuator is designed for power adjustment when the electromagnetic waves transmit through the main waveguide. The wavemeter was mounted on the reflectometer to find the coarse resonant frequency of the reflex klystron. The microwave cylindrical cavity was designed for the electromagnetic waves of  $\text{TM}_{010}$  mode and used as a probe in investigating the interaction of microwaves with materials in the cavity. Detailed discussion on each part of the units and the block diagram for the experimental apparatus (Fig. 2-11) follow.

#### Directional Coupler and Reflectometer

A directional coupler is a device used to divide microwave power. Two directional couplers were used in this investigation.

One leads microwave power to the frequency measuring section of the waveguide system which consists of a crystal diode detector that mixes and multiplies the frequency

reference signal. The directional coupler may be used to isolate signal sources or frequencies. Practically, the microwave power flowing into one (the forward) direction of the main waveguide is coupled to the r-f signal from the frequency standard. In this case, the directional coupler permits a sampling of the power from the microwave source, without any reflected waves, reaching the monitor. The reflectometer is exactly the same device as a directional coupler except that its usage is different. A reflectometer was coupled to the main waveguide, arranged to measure the incident and reflected voltages and to indicate their ratio. It serves to monitor the power when the microwaves are reflected from the cavity either loaded by the sample or unloaded. The reflected signal is detected by the crystal diode installed in the reflectometer. The output is amplified and recorded along with the frequency markers on a chart recorder. For recording the output data, a Hewlett-Packard Model 175A dual-trace oscilloscope was employed. One output went to the recording of the resonance shape and the other was connected to the marker system. The principle and design of the directional coupler is more completely discussed in "Microwave Spectroscopy".<sup>20</sup>

#### Wavemeter

The Narda Model 810 wavemeter was employed in this experiment for the purpose of the coarse frequency measurement.

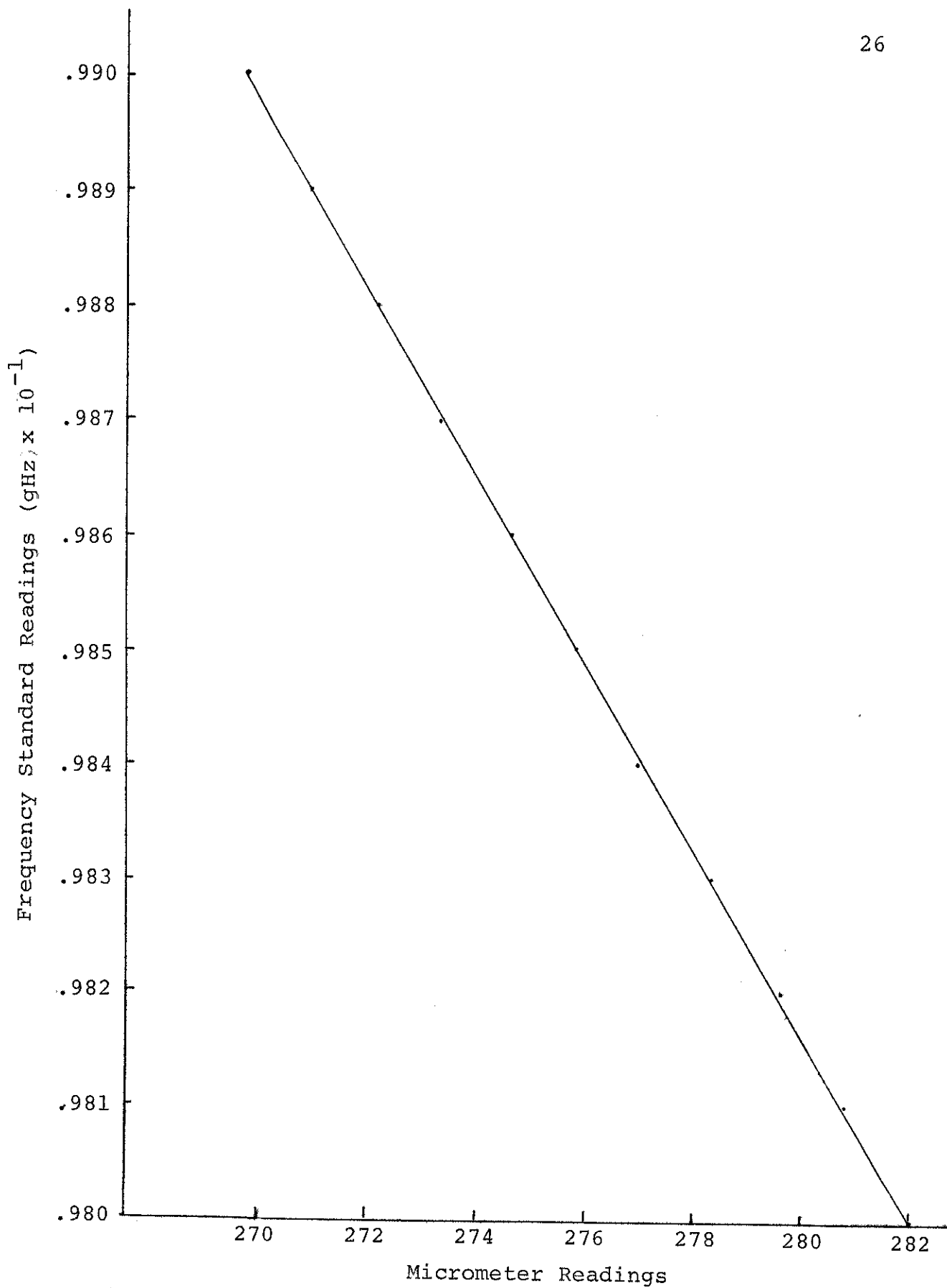


Fig. (2-6) Calibration curve for Narda Model 810 Wavemeter calibrated to General Radio Standard 1112A and 1112B.

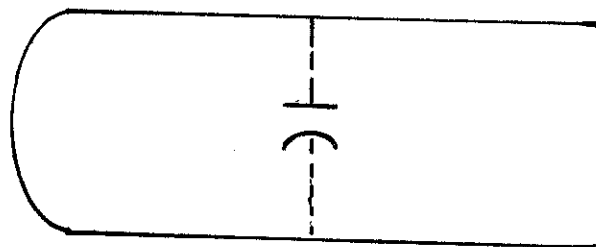
The calibration curve for the Narda Model 810 wavemeter was made by using the General Radio Standard Models 1112A and 1112B. Fig. (2-6) shows the calibration curve for the Narda Model 810 Wavemeter.

### Determination of Cylindrical Cavity Size, Operating Mode and Cavity Q Factor

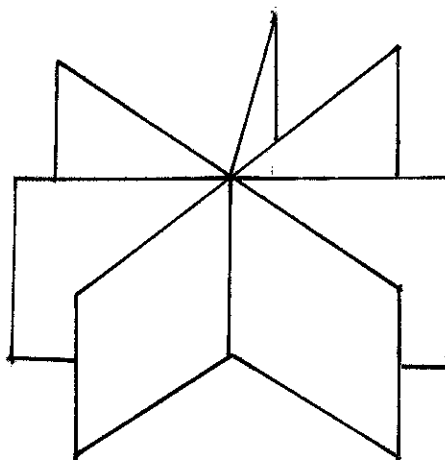
#### Principle of Cavity Resonator

The ordinary tuned circuit consists of a coil and a capacitor. The coil and capacitor are connected either in series or in parallel and have a resonant frequency given by  $f = 1/\sqrt{LC}$ . In order to increase the resonant frequency, it is necessary to reduce either the capacity or the inductance or both. The highest resonant frequency which can be obtained in such a way is that the inductance can be reduced to a half-turn coil and the capacitor reduced to only the stray capacity in the coil. A simple circuit as shown in Fig. (2-7-i) is not a proper design since ordinary circuits require high current handling capacity and high voltage breakdown insulation. The current handling capacity of a resonant circuit can be increased by adding half turn loops in parallel as shown in Fig. (2-7-ii). Addition of half turn loops does not affect the resonant frequency appreciably since the parallel inductance increases the the frequency and parallel capacity lowers the frequency. Therefore, the actual resonant frequency remains about the

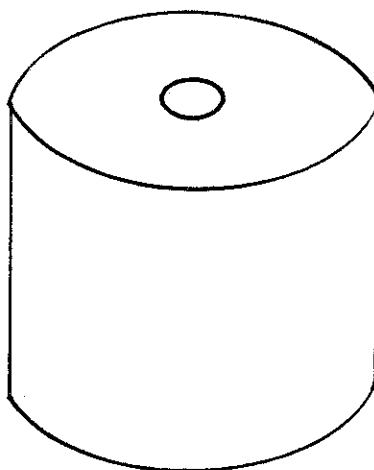




(i) Simplest tuned circuit



(ii) Half turns in parallel



(iii) Resonant cavity

Fig. (2-7) Various types of tuned circuits

same. By adding more and more loops, the resonant cavity can be formed as shown in Fig. (2-7-iii).

Further discussion of the wave functions subject to the cavity boundary condition for a cavity operating  $TM_{010}$  mode and experimental techniques for obtaining the cavity size and geometry were give in Ref. 17,21. The operating mode can be uniquely determined from the boundary condition of the probing cavity. In order to get the localized electric fields, the  $TM_{010}$  mode is the most suitable mode for our investigation.

#### Cavity Q Determination

The definition of  $Q$  is a measurement of sharpness of response of the cavity to external excitation. A mathematical expression for  $Q$  is given as

$$Q = \frac{\omega_0 \text{ stored energy}}{\text{energy loss}} \quad (2-5)$$

where  $\omega_0/2\pi$  is the resonance frequency. The resonance profile of the cavity  $Q$  was shown to be Lorentzian shape (Ref. 18) and Eq. (2-5) may be converted to the useful expression for the determination of the cavity  $Q$ .

In order to determine the cavity  $Q$ , the exact resonant frequency of the unloaded cavity must be measured. In this experimental operation, the resonant frequency of the cavity was 9.927 kHz. In order to get half power reading from a power absorption line shape, a 42 kHz modulation frequency

was used to differentiate the absorption signal. The frequency reading for half-width of the resonant shape was 0.824 kHz. In order to find the actual frequency of the half-width, the correction equation (Eq. 2-2) must be applied to correct the modulation.

In order to obtain the best values, the half-width was measured more than ten times and averaged. The inner surface of the cavity was coated with silver to reduce the Ohmic loss due to the current flowing inside the walls of the cavity. Therefore, the silver coating leads to a higher Q value than that for the copper foundation material.

#### Field Pattern for $TM_{010}$ Mode

Solving Maxwell's frequency dependent field equations, in cylindrical resonant cavity for the  $TM_{010}$  mode, yields solutions for  $\vec{E}$  and  $\vec{H}$  which can be expressed as follows (Ref. 21)

$$E_z = \frac{cK}{(4\pi\sigma + j\omega\epsilon)} AJ_0(Kr)e^{j\omega t} \quad (2-6)$$

$$H_\theta = AJ_1(Kr)e^{j\omega t} \quad (2-7)$$

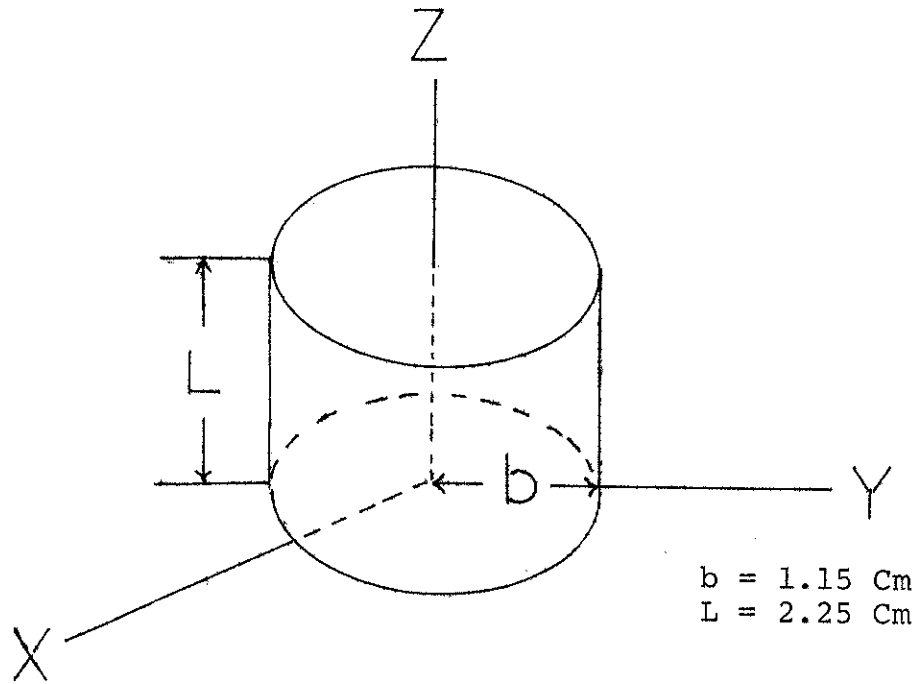
in which  $J_0$  and  $J_1$  are the Bessel functions of the first kind, A is a constant governed by the field strength of excitation and K is propagation constant. The electromagnetic fields for  $TM_{010}$  mode in the cavity are determined by referring to

Eq. (2-6) and Eq. (2-7) which include Bessel functions of the first kind. There is no other component except for  $E_z$  and  $H_\theta$  for  $TM_{010}$  mode in the cylindrical cavity.

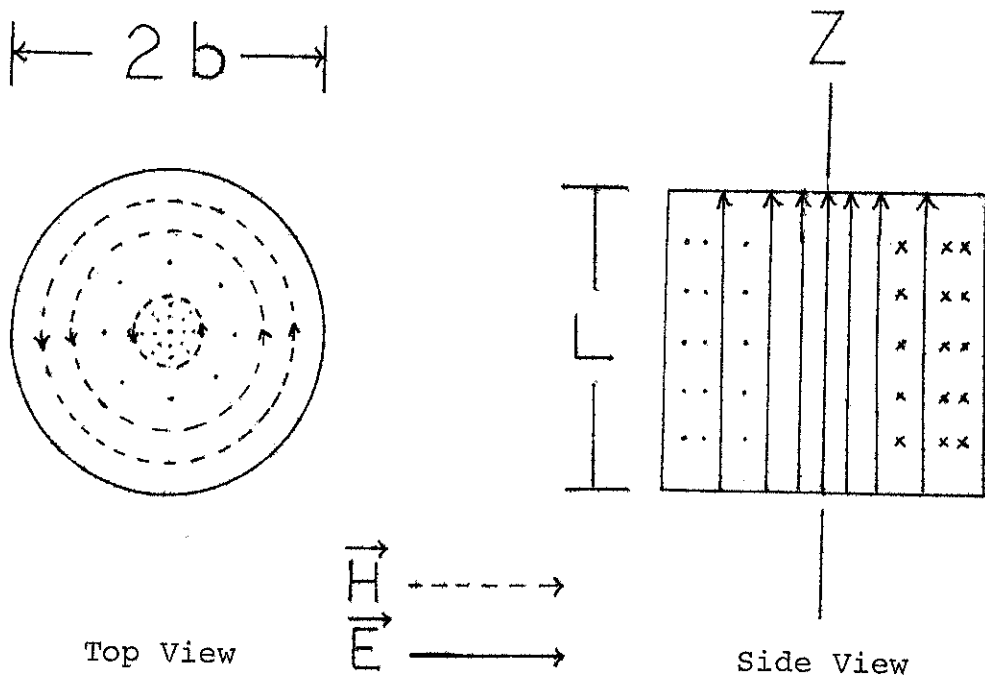
Actual field patterns in the cylindrical cavity for  $TM_{010}$  mode are drawn in Fig. (2-8-ii).

The electric field intensity has its maximum value at  $r = 0$ , whereas the magnetic field is zero at the Z-axis as shown in Fig. (2-9-i). As the radius increases toward the cavity boundary, the electric field intensity becomes zero at the cavity wall while the magnetic field intensity increases to its maximum value and reaches a definite value at the cavity wall as  $r$  goes to  $r = b$ . Near the Z-axis, the magnetic field intensity can be neglected since the electric field intensity is much larger than the magnetic field. Therefore, it is obvious that the  $TM_{010}$  mode has more advantages than any other modes in studying electric field interaction with materials placed coaxially within the cylindrical cavity.

The actual electric field pattern at  $r = 0$  is slightly altered when the circular iris is drilled at the center of the end face<sup>22</sup>. A circular hole drilled at the center of the end face distorts the electric lines of force in a manner which suggests the presence of an electric dipole. The magnetic dipole moment is equal to zero at the circular hole. Fig. (2-9-ii) shows the exaggerated electric field lines in a circular cylindrical cavity with a central hole.

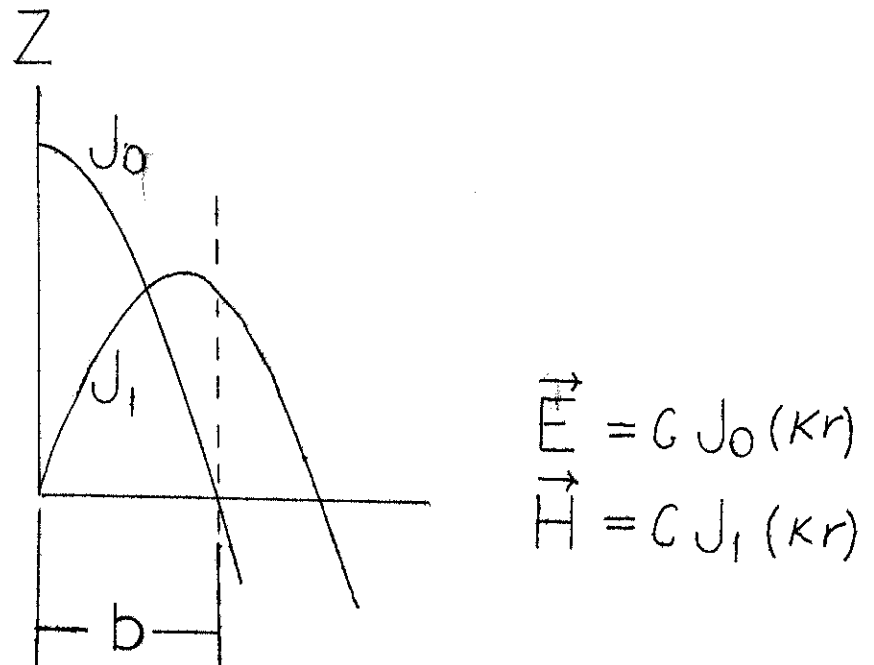


(i) Cylindrical cavity size for  $TM_{010}$  Mode

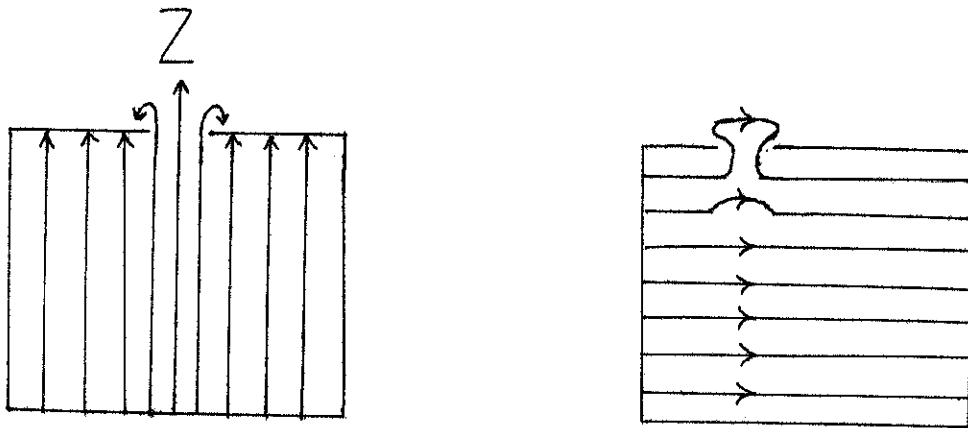


(ii) Field pattern for  $TM_{010}$  Mode

Fig. (2-8) Microwave cavity geometry



(i) Electromagnetic field intensity from side of the cavity.



(ii) Lines of  $\vec{E}$  in a cylindrical cavity with central and side iris holes.

Fig. (2-9) Electromagnetic field intensity and field distortion around the iris holes.

Another important consideration is to investigate the field lines at the sample boundaries. Actually, it is difficult to discover precisely how the electric field behaves at the sample boundaries when the oscillating electric field is applied.

There are many factors to change the field configuration. The iris position, the dielectric sample insertion into the resonant cavity and the variation of the iris diameter cause the field pattern around them to change. The details of the disturbance due to the change of boundary conditions of the cavity will be discussed in Chapter III.

Sample Driving Micrometer, Measurement of  
Perturbation and Normalization  
of the Perturbing Sample

The cylindrical cavity was constructed to investigate microwave properties of liquids and solids. The cavity was specially designed for  $TM_{010}$  mode with the resonant frequency 9.927 kHz. In one of the top cylinder faces, there is a sample inserting hole (diameter = 0.172"), with a micrometer drive installed for insertion of the test sample as shown in Fig. (2-10). The sample can be inserted coaxially into the cavity and each scale reading of the micrometer can be adjusted up to  $10^{-3}$  cm. Diameters of the samples were carefully measured by using a microscope. Diameters of cylindrical samples used in this experiment are listed in Appendix IV and the behavior of each sample will be discussed

in Chapter III. Careful attention had to be paid to the normalization of the sample volume and the resonant frequency shift. Before the sample was inserted into the cavity, a very thin piece of paper was placed on top of the sample inserting hole of the cavity in order to make sure that the zero reading of the micrometer drive was established to be the same for each sample. Magnifying lenses were used to obtain the most accurate reading for different trials.



Fig. (2-10)

Cavity geometry employed for sample probing into the  
microwave cavity.

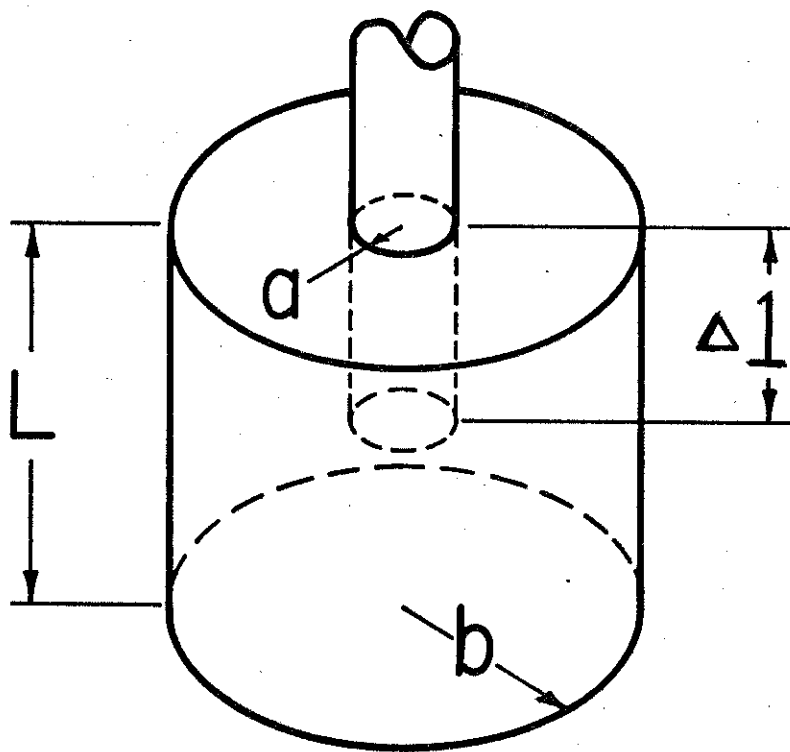
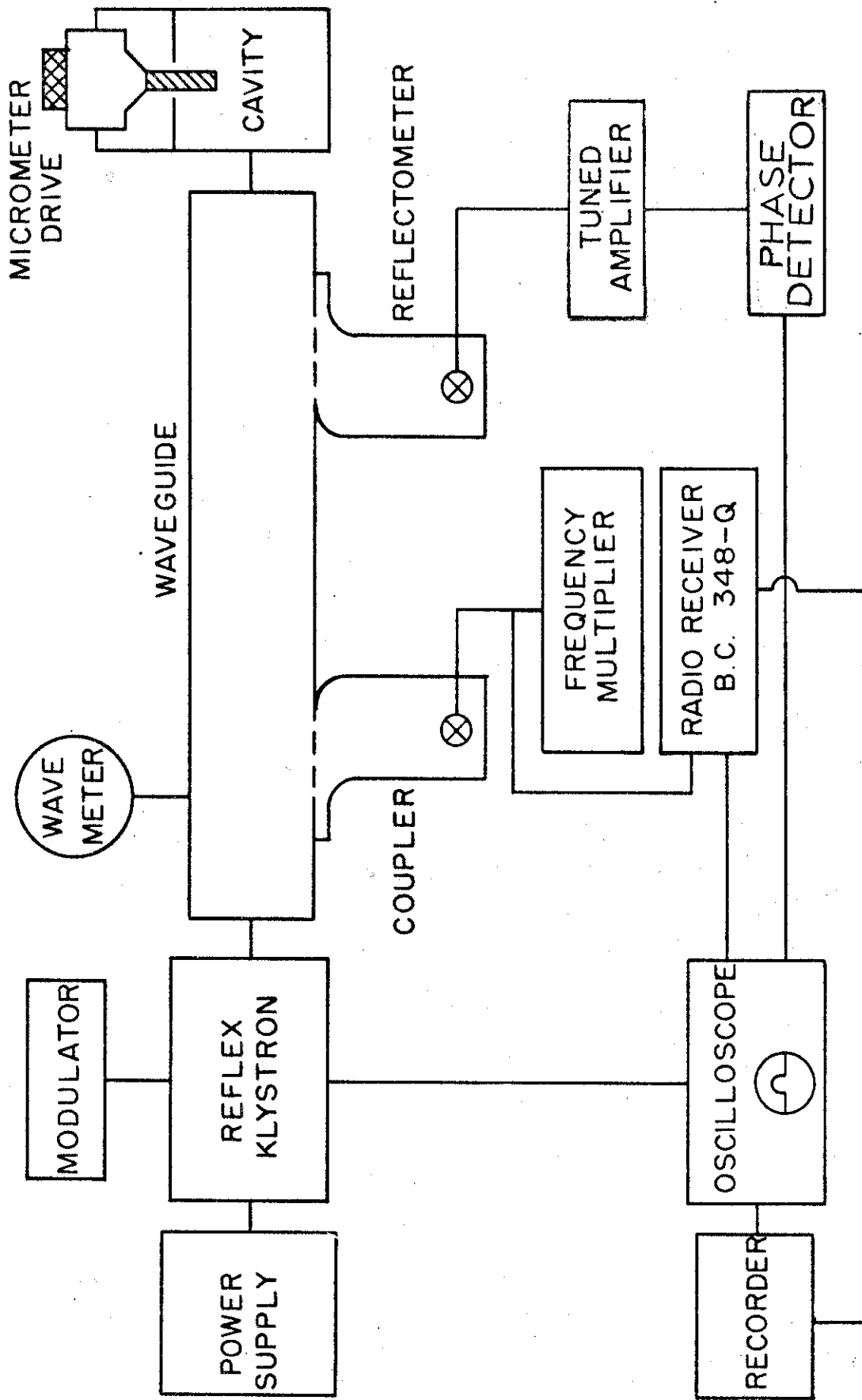


Fig. (2-11)

Block diagram of the experimental arrangement employed  
make this investigation.



EXPERIMENTAL ARRANGEMENT

## CHAPTER III

### SUMMARY OF RESULTS

The treatment in this paper led to results for  $Q$  change and resonant frequency shifts vs. perturbation volume increment which are related to equations which were used to deduce complex dielectric constants. Experimental results were obtained and compared with the predicted behavior of  $Q$  and  $\Delta f/f$  for the  $TM_{010}$  mode using the perturbation equations for a resonant cavity.

Since this investigation relies on the perturbation theory, Slater's perturbation theory is introduced before extensive discussion of the data is given.

Following Slater, the complex dielectric constant can be measured by observing the change in resonant frequency and  $Q$  of the cavity as the cavity is perturbed by a known volume of the sample to be studied.

For a rod placed parallel to the electric field, the perturbation theory gives<sup>5</sup>

$$\frac{\Delta f}{f} - j\Delta\left(\frac{1}{Q}\right) = \frac{-\int_v (\epsilon' - 1 - j\epsilon'') E^2 dv}{2\int_v E^2 dv} \quad (3-1)$$

where  $\Delta f$  is the resonant frequency shift due to the perturbation volume  $v$ ,  $Q$  the quality factor relating to resonant half width  $w$ ,  $\epsilon'$  and  $\epsilon''$  are the real and imaginary parts of

the complex dielectric constant,  $V$  is the cavity volume, and  $E$  is the electric field in the cavity. It should be noted that the electric field  $E$  is assumed to depart only slightly from the unperturbed field when a sample is placed in the cavity. Also, the probing sample volume must be much smaller than the cavity volume.

For an unperturbed cavity, the electric field for the  $TM_{010}$  mode is given by (Ref. 21)

$$E = DJ_0\left(K\frac{r}{b}\right) \quad (3-2)$$

where  $K$  is a propagation factor and  $D$  is a constant.

The samples were of radii  $a$  and were inserted incrementally down the axis of the cavity with the resultant frequency shift and  $Q$  change observed. Under the experimental conditions, the integrals had to be evaluated for a cavity geometry as shown in Fig. (2-10). The integral may be expressed as

$$\frac{\Delta f}{f} = \frac{\int_0^a \int_0^{\Delta l} \int_0^{2\pi} (\epsilon' - 1) E^2 r dr d\phi dz}{2 \int_0^b \int_0^L \int_0^{2\pi} E^2 r dr d\phi dz} \quad (3-3)$$

and

$$\Delta\left(\frac{1}{Q}\right) = \frac{\int_0^a \int_0^{\Delta l} \int_0^{2\pi} \epsilon'' E^2 r dr d\phi dz}{\int_0^b \int_0^L \int_0^{2\pi} E^2 r dr d\phi dz} \quad (3-4)$$

where  $\epsilon''$  is the lossy part of the dielectric constant and the ratio of  $\epsilon''/\epsilon'$  is defined as the loss tangent<sup>1</sup> and  $\Delta l$  is incremental length of the liquid sample.

It is clear from this investigation that the nature of the E field in the vicinity of the iris through which the sample was admitted cannot be linearly related to the unperturbed field although Eq. (3-3) and Eq. (3-4) require such a behavior. Moreover, the nature of the field within the sample itself is changing in non-simple way.

Both the nature of the field near the iris<sup>23</sup> and the nature of the field within the sample have been explored by other investigators.<sup>15</sup>

The microwave parameters were explored for the best consistency between the Q change and resonant frequency shift equations. The results of this process led to a linear relationship between  $\Delta l$  and  $\Delta f$  which yielded the real part of the electric susceptibility. Likewise the results for  $\Delta l$  vs.  $\Delta(1/Q)$  yielded the damping term of the electric susceptibility.

When the cavity perturbation technique is employed, accurate measurements of frequency and the sample dimensions are very important in determining dielectric parameters. In past works, common experimental difficulties of the cavity method have required that one merely neglect the iris effect although the iris terms are shown to be important in this work and are known from the perturbation theory to be important. In most cases of determining dielectric constants, the sample was coaxially placed through the cavity. In those cases, the cylinder cavity has two irises, one at each cylinder end face.

Since accurate frequency shift due to the presence of the sample volume in an unperturbed field is of vital importance in determining dielectric constants, compensation for the effect is desired to determine the resonant frequency shift. The present experiment was performed in order to observe the actual experimental iris effects and to determine how to remove the iris effect such that accurate measurement of the resonant frequency shift can be determined and hence dielectric constants determined by the cavity perturbation method.

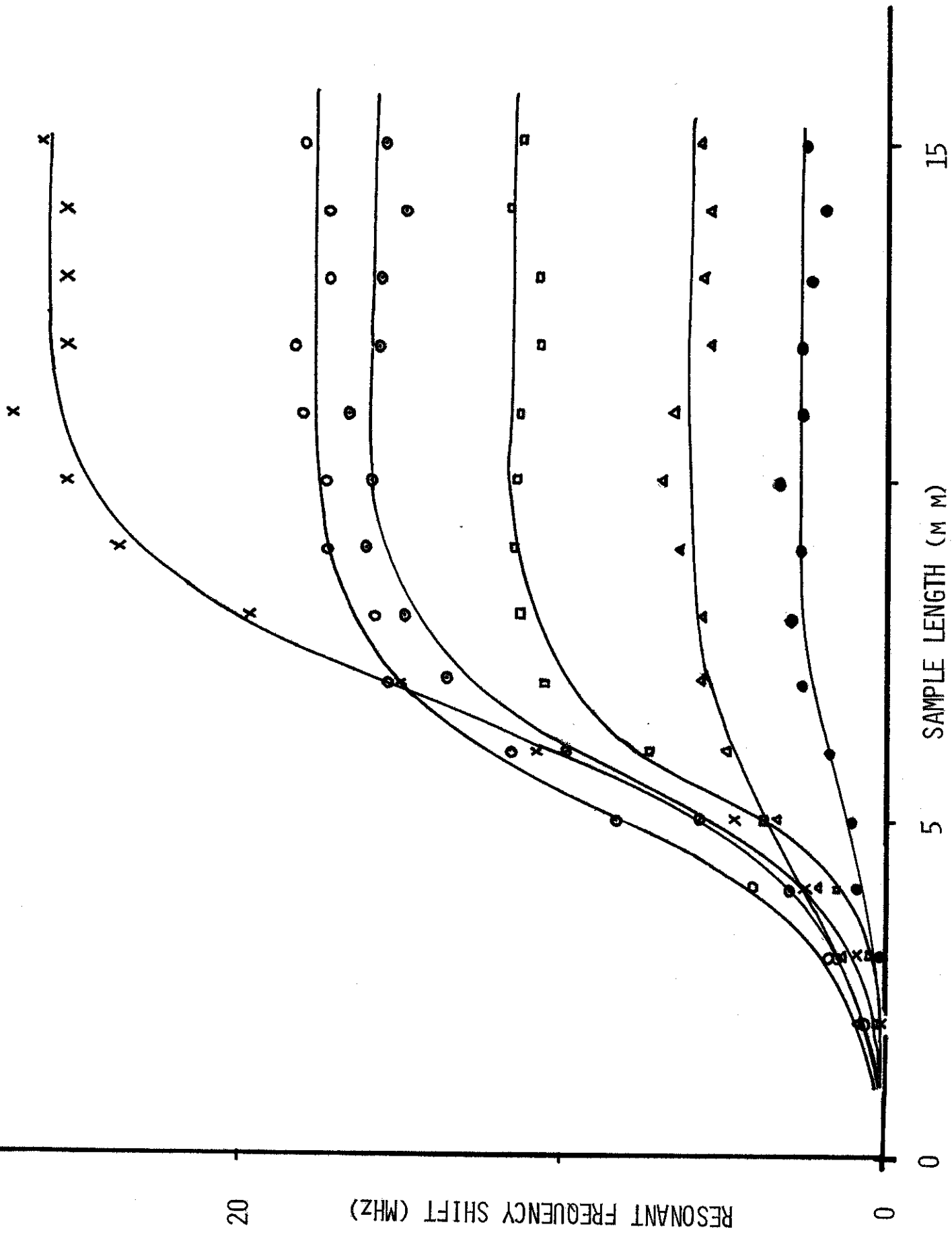
In this experiment, a thin-walled teflon tube whose diameter is 1.5 mm was employed as a liquid container. If a container is used, it must be determined whether the summation of the resonant frequency shifts of the container and the material in the container are linearly additive. Appendix II shows that the frequency shifts are linearly additive to an accuracy of 5%.

Incremental samples of liquid were introduced into the teflon tubes, and the sample was advanced into the cavity. The resonant frequency shift due to the liquid was obtained by subtracting the frequency shift of the teflon carrier tube from the total resonant frequency shift for each depth of penetration. For different volumes of liquid, the resonant frequency shifts were plotted. Fig. (3-1) shows plots of teflon carrier depth with several benzene volumes vs. resonant frequency shift. As the sample sufficiently



Fig. (3-1)

Behavior of resonant frequency shift vs. various amounts of benzene admitted into the resonant cavity along its symmetry axis. Bold lines are drawn for clarity.



penetrates into the cavity, the resonant frequency shift tends to a constant value. The constant value of resonant frequency shift for given volume means that the sample is no longer in the region of iris effect. A plot of these incremental volumes vs. frequency shift gives a parameter which is related to the dielectric constant of the material. As shown in Fig. (3-1), the iris effect is important up to a sample depth of  $\sim 10$  mm. Therefore, we need to find the region where the iris effect is negligibly small so that the frequency shift measurements can be made completely out of the iris region.

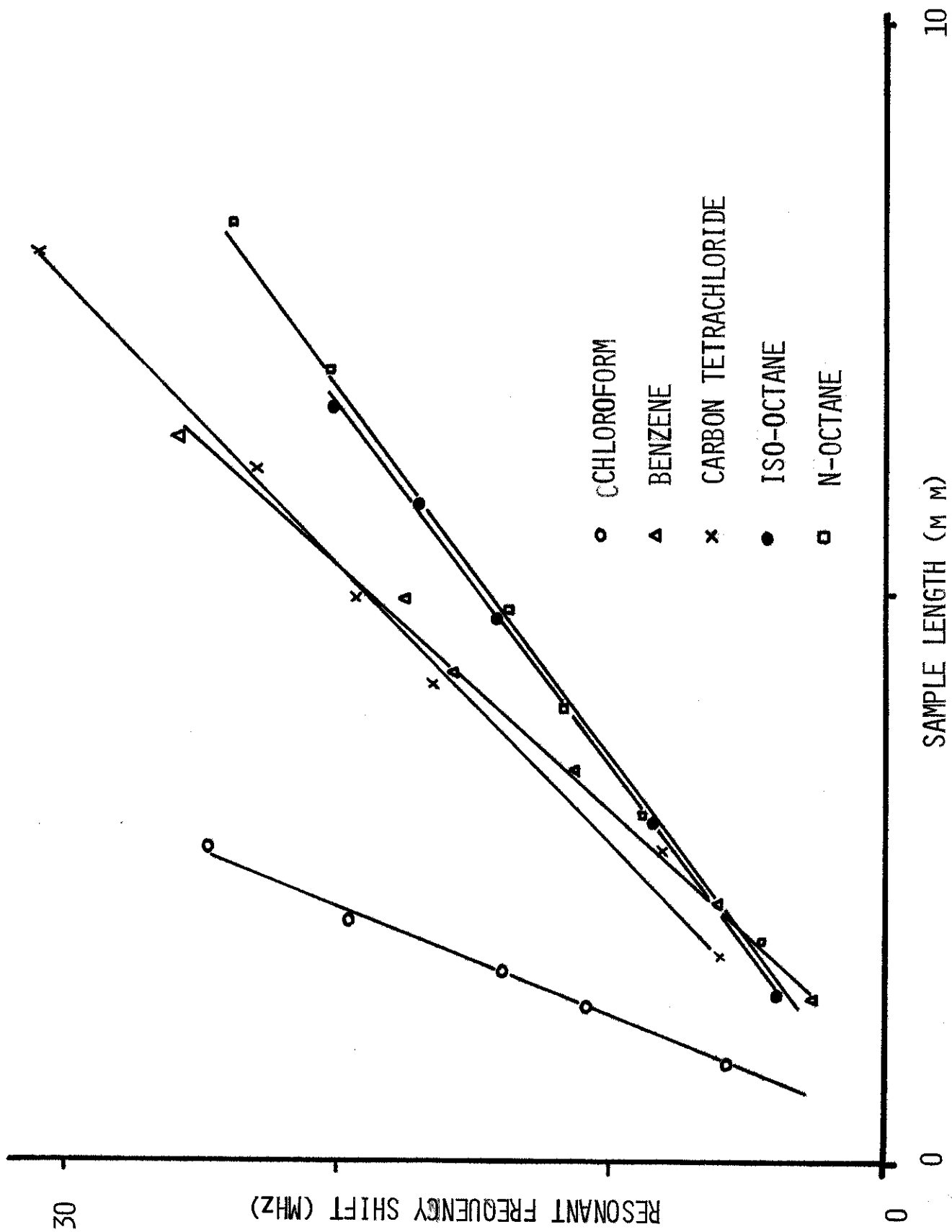
The same technique was applied to other non-polar liquid samples. After accounting for the iris effect, liquid volume vs. resonant frequency shift can be plotted. The plot for  $\Delta l$  vs.  $\Delta f$  in which the iris effect was removed gives more accurate frequency measurement for the sample than the conventional cavity method.

Fig. (3-2) shows a plot of  $\Delta l$  (liquid depth in the teflon tube which is proportional to liquid volume) vs.  $\Delta f$  for various liquids. The graph shows that  $\Delta l$  is linearly proportional to  $\Delta f$  for most liquids employed. With these experimental data, a linear least square fit was employed and slope parameters were deduced from them.

Once the iris effect was accounted for, dielectric constants using the perturbation equation of Slater were obtained.

Fig. (3-2)

Resonant frequency shifts vs. various liquid sample volumes after iris effect has been removed from the experimental data. (Bold lines represent least square fit to a linear function.)



Applying our experimental geometry dimension to Eq. (3-3), the final form of the dielectric constant equation is given by

$$\epsilon' = 1 + .28S \quad (3-5)$$

where  $S = \frac{\Delta f}{\Delta l}$  is the slope parameter from Fig. (3-2). The slope parameter along with the  $\epsilon'$  calculated from them are given in Table II.

Furthermore, dielectric constants of low loss solids were calculated by a direct application of the perturbation equation. These solid samples could be admitted far into the cavity. The total resonant frequency shift for a given sample volume was measured. (See Appendix III) Using Eq. (3-3), dielectric constants of solids were calculated to deduce Table II.

In addition to obtaining dielectric constants for the sample, loss tangents were observed. The loss tangent may be calculated by taking the ratio of Eq. (3-3) to Eq. (3-4). For the same sample geometry, an equation which may be used to obtain loss tangents of a material using the method is given by

$$\frac{2\epsilon''}{(\epsilon' - 1)} = \frac{\Delta w}{\Delta f} \quad (3-6)$$

where  $\Delta w$  is width of the resonance at half-power points. The values of  $\Delta w$  and  $\Delta f$  for each volume increment were measured as the sample was inserted along the cylindrical axis of the cavity. The results are shown in Fig. (3-3).

TABLE II

EXPERIMENTAL VALUES OF MICROWAVE PARAMETERS  
FOR LIQUIDS AND SOLIDS

Samples	Slope Parameter S	$\epsilon'$ (literature)	$\epsilon'$	$\epsilon''/\epsilon'$ (literature)	$\epsilon''/\epsilon'$
Chloroform	10.15	4.81 <sup>a</sup>	3.88		.052
Carbon Tetrachloride	4.13	2.17 <sup>b</sup>	2.17		.0009
N-octane	3.03	1.92 <sup>c</sup> , 1.94 <sup>d</sup>	1.86		.004
Iso-octane	3.13	1.92 <sup>c</sup> , 1.94 <sup>d</sup>	1.89		.06
Benzene	4.70	2.28 <sup>e</sup>	2.31		.0007
Teflon		2.08	2.01	$2 \times 10^{-4b}$	$10^{-5}$
Quartz		3.78 <sup>b</sup>	3.45	$4 \times 10^{-4b}$	$10^{-5}$
Cu <sub>2</sub> O		(7.6 - 6.4) <sup>e</sup>	2.91 <sup>f</sup>		.056
Cu O		18.1 <sup>d</sup>	11.2		.022
Na Cl		5.9 <sup>a-e</sup>	4.53	$5 \times 10^{-4b}$	$<10^{-5}$

TABLE II -- Continued

Values (a-d) were obtained from Dielectric Materials and Applications, Arthur R. Von Hippel, Editor, Technology Press of M.I.T. and J. Wiley & Sons, N.Y. (1954).

Frequencies are given as follows:

a. Static

b.  $10^{10}$  Hz

c.  $3 \times 10^9$  Hz

d.  $3 \times 10^8$  Hz

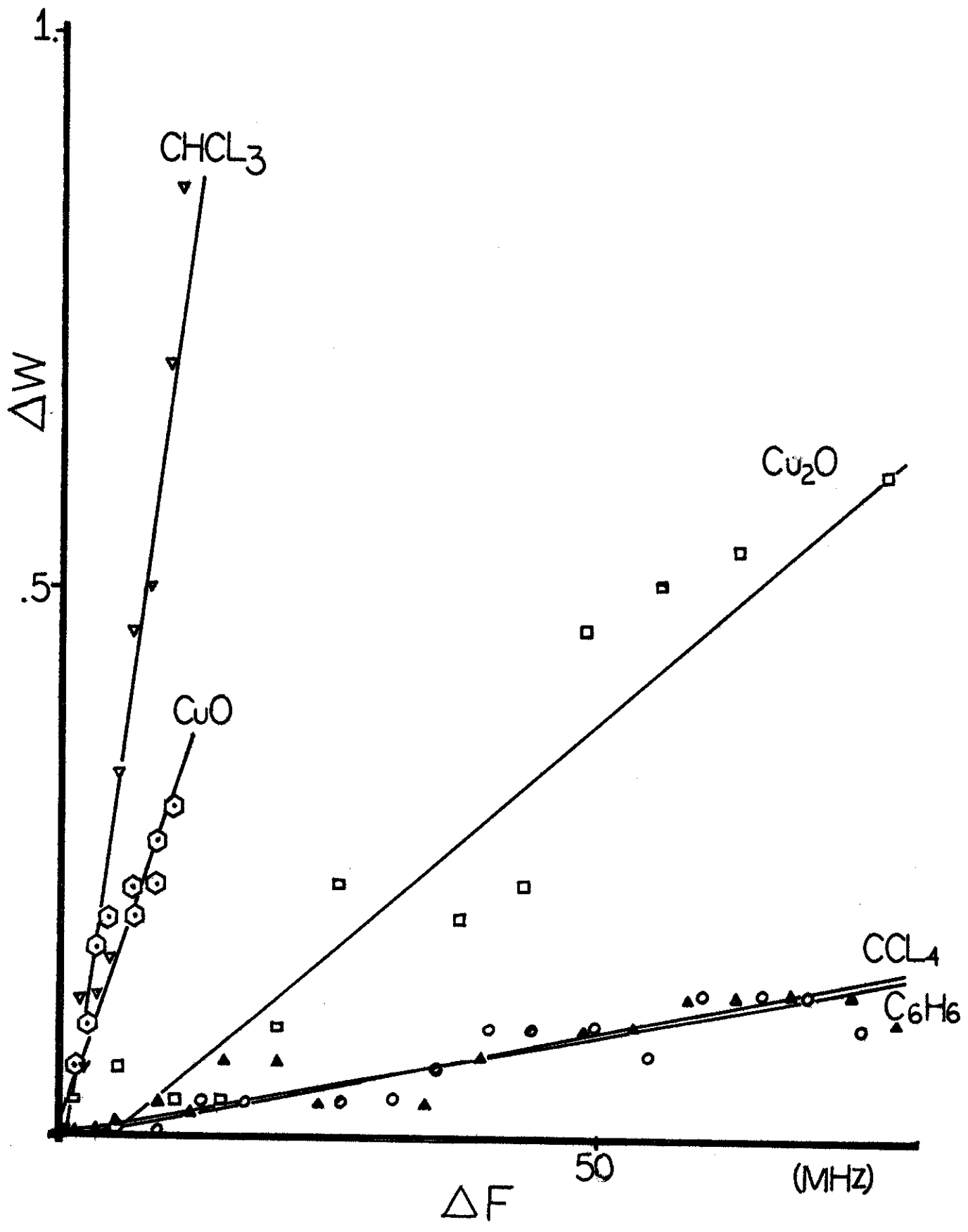
e. R. Kuzel and F. L. Weichman, Can. J. Phys. 48, 2648 (1970).

f. This value depended upon degree of packing. See G. P. Srivastava, P. C. Mathur, (Mrs.) Krishna and R. M. Mehra. Indian J. of Pure and Appl. Phys. 9, 453 (1971).



Fig. (3-3)

Experimental data for  $\Delta w$  vs.  $\Delta f$  to deduce loss tangents.  
Bold lines represent theoretical curve fittings.



Since the ratio of  $\Delta f$  vs.  $\Delta w$  is found to be linear, we have the following relation (with modulation correction)

$$\frac{\epsilon''}{\epsilon' - 1} = \frac{\sqrt{3}}{2} \frac{\Delta w}{\Delta f} \quad (3-7)$$

or

$$\tan \delta = \frac{\epsilon''}{\epsilon'} = .866 \frac{\Delta w}{\Delta f} \left(1 - \frac{1}{\epsilon'}\right) \quad (3-8)$$

where values of  $\frac{\Delta w}{\Delta f}$  can be obtained from Fig. (3-3). Loss tangents for liquids and solids obtained from Eq. (3-8) are listed in Table II.

Although the cavity resonant frequency was 10 GHz, our resonant frequency shift for the perturbation could be accurately measured  $\frac{1}{10^6}$  over range up to 100 MHz of the cavity frequency change. Hence, the numerical values for the frequency changes are valid up to  $\frac{\Delta f}{f} \sim .01$ . On the other hand, it is possible to measure the resonant half-width up to the order of .01 MHz, i.e.,

$$\frac{\epsilon''}{\epsilon'} \sim \frac{.01}{100} = .0001 \quad (3-9)$$

Therefore, the numerical value for loss tangents was assumed to be valid up to the order of  $\sim 10^{-4}$ .

The results of this investigation show that in order to obtain the most accurate measurements of dielectric constants by using the cavity method it is necessary to take into consideration all modes of energy losses within the resonant cavity. This paper dealt mainly with the iris

effect and energy losses due to its presence. It was shown that the presence of a single iris perturbs the cavity boundary to the extent that large errors are introduced in  $Q$  and resonant frequency parameters. In the resonant cavity experiments on plasmas it is necessary to have two irises. Recent work with plasma probing using cavities has shown the error introduced by two irises to be as much as 29% in number density measurements.<sup>24</sup> This work showed that errors may range from a few percent to one hundred percent if samples are probed in the iris region.

The results presented for the dielectric constant measurements with the iris effect removed are believed to be the most accurate available. The repeatability of the measurements of this work shows that dielectric constants and loss tangents can be repeatedly measured with an accuracy better than 5% for non-polar samples.

## APPENDIX I

## PHYSICAL DIMENSIONS OF SAMPLE

Sample	Diameter (mm)
Teflon tube	inner 1.50 outer 2.32
Quartz tube	inner 1.00 outer 2.10
Cupric oxide rod	.64
Sodium Chloride	1.09 x 1.70

## APPENDIX II

CHECK TO DETERMINE THE ADDITIVE PROPERTY OF  
THE RESONANT FREQUENCY SHIFTS USING TWO  
DIFFERENT RADII QUARTZ TUBES

In order to ascertain the nature of the summation of the resonant frequency shifts of the material and its container, two different radii of quartz tubes were employed, one of which could be inserted into the other.

The two tubes were designated by the small radius quartz tube "Q(1)" and the large radius quartz "Q(2)". In this case, three different observations for the sample penetration depth vs. the resonant frequency shifts were made as follows:

1.  $(\Delta l)Q(1)$  vs.  $\Delta f(1)$
2.  $(\Delta l)Q(2)$  vs.  $\Delta f(2)$
3.  $(\Delta l)Q(1)$  plus  $Q(2)$  vs.  $\Delta f(3)$

where  $\Delta l$  is the sample penetration depth and  $\Delta f$  is the resonant frequency shift due to the perturbation.

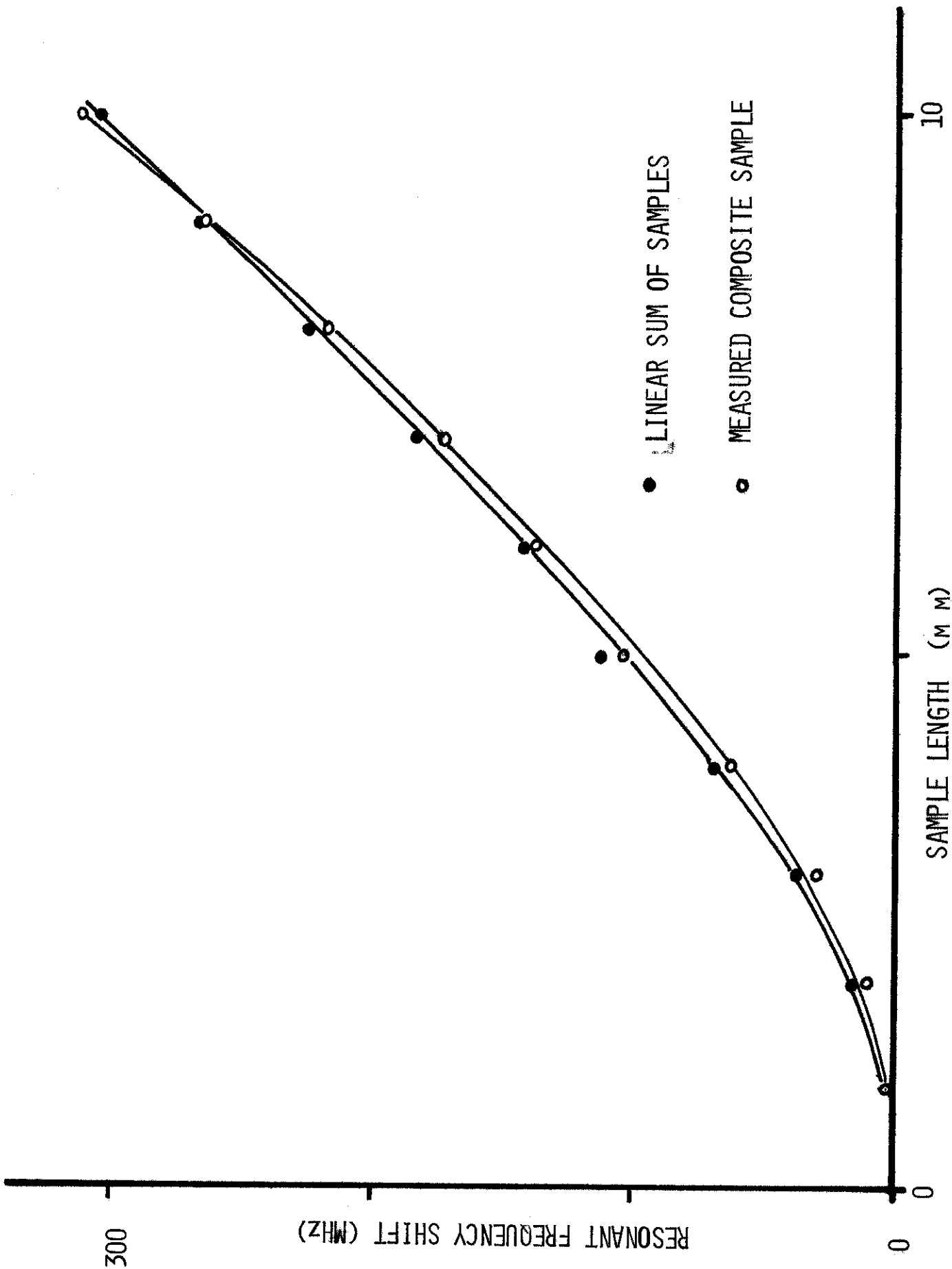
For given sample depth,  $\Delta f(1)$  of Q(1) and  $\Delta f(2)$  of Q(2) was added and compared with the direct measurement of  $\Delta f(3)$  of two tubes together. These two values of  $\Delta f(1) + \Delta f(2)$  and  $\Delta f(3)$  vs.  $\Delta l$  are plotted in Fig. (A-I). This experiment indicated the frequency shifts were linearly additive to an accuracy of 5 per cent. In additional

experiments with dissimilar materials the linear property of frequency shifts was not as good. The error was observed to be as much as 6.5 per cent.

Fig. (A-1)

Check for additive property of the resonant frequency shifts using two different radii quartz tube. (Bold lines represent theoretical least square fit curves.)





## APPENDIX III

## EXPERIMENTAL DATA FOR SOLIDS STUDIED

Sample	Sample Depth (mm)	Resonant Frequency Shift (MHz)
Teflon	22.5	118
Quartz	13.5	170
$\text{Cu}_2\text{O}$	10	31.8
$\text{CuO}$	4.8	11.5
Na Cl	6	51.6

## REFERENCES

- <sup>1</sup>A. V. Hippel, Dielectrics and Waves (John Wiley & Sons, Inc., New York, 1954).
- <sup>2</sup>Curtis C. Johnson, Field and Wave Electrodynamics (McGraw-Hill Book Co., New York, 1965).
- <sup>3</sup>J. Basu and C. Dutta, "Microwave Determination of Electron Density Distribution in a Plasma," J. Inst. Telecom. Engrs., 20, 510 (1965).
- <sup>4</sup>H. A. Bethe and H. Schwinger, N.D.R.C. Report DI-117 (Cornell University, March, 1945).
- <sup>5</sup>J. C. Slater, Rev. Mod. Phys. 18, 441 (1946).
- <sup>6</sup>F. Horner, R. A. Taylor, R. Dunsmuir, J. Lamb and Willis Jackson, J. Inst. Elec. Engrs. 93, 53 (1946).
- <sup>7</sup>L. C. Maier, Jr. and J. C. Slater, J. Appl. Phys. 23, 68 (1952).
- <sup>8</sup>J. N. Bhar, Proc. IEEE. 51, 1623 (1963).
- <sup>9</sup>E. Gerdes, W. D. Kraeft and M. Zecha, Zeitschrift für Physikalische Chemie 241, 25 (1969).
- <sup>10</sup>G. P. Srivastava, P. C. Mathur, (Mrs.) Krishna and R. M. Mehra, "Dielectric Measurements on Alloy Semiconductors in the Microwave Frequency Region," Indian J. of Pure and Applied Phys. 9, 453 (1971).
- <sup>11</sup>E. G. Spencer, R. C. LeCraw and L. A. Ault, J. Appl. Phys. 28, 130 (1957).
- <sup>12</sup>J. E. Tompkins and E. G. Spencer, J. Appl. Phys. 28, 969 (1957).
- <sup>13</sup>I. P. Kaminow and G. O. Harding, "Complex Dielectric Constant of  $\text{KH}_2\text{PO}_4$  at 9.2 GHz," Phys. Rev. 129, 1562 (1963).
- <sup>14</sup>S. K. Sen, J. Basu and A. K. Ghosal, Indian J. Appl. Phys. 38, 55 (1964).
- <sup>15</sup>Z. Haniotis and H. H. Günthard, Z. Angew Math Phys. 20, 771 (1969).

- 16 Richard B. Hall, J. Appl. Phys. 40, 30 (1969).
- 17 E. L. Ginzton, Microwave Measurements (McGraw-Hill Book Co., New York, 1957).
- 18 R. P. Netterfield, R. W. Parsons and J. A. Roberts, J. Phys. B: Atom. Molec. Phys., 5, 146 (1972)
- 19 E. A. Rinehart, R. L. Legan and C. C. Lin, Rev. Sci. Instr. 36, 511 (1965).
- 20 C. H. Townes and A. L. Schawlow, Microwave Spectroscopy (McGraw-Hill Book Co., New York, 1961).
- 21 R. F. Harrington, Time-Harmonic Electromagnetic Fields (McGraw-Hill Book Co., New York, 1961).
- 22 J. V. Bladel, Electromagnetic Fields (McGraw-Hill Book Co., New York, 1964).
- 23 G. Goubau, Electromagnetic Waveguides and Cavities (Pergamon Press, New York, 1961).
- 24 A. Pipiskova and P. Lukac, J. Phys. D: Appl. Phys. 3, 1381 (1970).

## BIBLIOGRAPHY

### Books

- Bladel, J. V., Electromagnetic Fields, New York, McGraw-Hill Book Co., 1964.
- Fröhlich, H., Theory of Dielectrics, Oxford, Oxford University Press, 1950.
- Ginzton, E. L., Microwave Measurements, New York, McGraw-Hill Book Co., 1957.
- Goubau, G., Electromagnetic Waveguides and Cavities, New York, Pergamon Press, 1961.
- Harrington, Roger F., Time-Harmonic Electromagnetic Fields, New York, McGraw Hill Book Co., 1961.
- Hippel, A. V., Dielectrics and Waves, New York, John Wiley & Sons, Inc., 1954.
- Jackson, John D., Classical Electrodynamics, New York, John Wiley & Sons, Inc., 1962.
- Johnson, Curtis C., Field and Wave Electrodynamics, New York, McGraw-Hill Book Co., 1965.
- Kittel, Charles, Introduction to Solid State Physics, New York, John Wiley & Sons, Inc., 1966.
- Sands, M., R. B. Leighton, and R. P. Feynman, Lectures on Physics, Vol. II, Massachusetts, Addison-Wesley Publication Co., Inc., 1964.
- Townes, C. H. and A. L. Sehallow, Microwave Spectroscopy, New York, McGraw-Hill Book Co., 1955.
- Zaky, A. A. and R. Hawley, Dielectric Solids, New York, Dover Publications, Inc., 1970.

### Articles

- Basu, J. and C. Dutta, "Microwave Determination of Electron Density Distribution in a Plasma," J. Inst. Telecom. Engrs., 20 (September, 1965), 510-514.

- Bhar, J. N., "Microwave Techniques in the Study of Semiconductors," Proc. IEEE., 51 (November, 1963), 1623-1631.
- Gerdes, E., W. D. Kraeft and M. Zecha, "Messung der Komplexen Dielectrizitätskonstanten von Ionenlösungen mittels Hohlraumresonatoren bei 3.2 Cm Wellenlänge," Zeitschrift für Physikalische Chemie, 241 (March, 1969), 25-32.
- Hall, Richard B., "Perturbation of Microwave Cavities by Lossy Dielectrics and Plasma," J. Appl. Phys., 40 (January, 1969), 30-36.
- Haniotis, Zeppos and H. Hans Günthard, "Frequency Shift and Q Deterioration of the  $TE_{011}$  Cylindrical Cavity by Coaxial Loading with a Scalar Dielectric," Z. Angew Math. Phys., 20 (February, 1969), 771-780.
- Horner, F. T. A. Taylor, R. Dunsmuir, J. Lamb and Willis Jackson, "Resonance Methods of Dielectric Measurement at Centimeter Wavelengths," J. Inst. Elec. Engrs., 93 (October, 1946), 53-68.
- Kaminow, I. P. and G. O. Harding, "Complex Dielectric Constant of  $KH_2PO_4$  at 9.2 GHz," Phys. Rev., 129 (February, 1963), 1562-1566.
- Maier, L. C. and J. C. Slater, "Field Strength Measurements in Resonant Cavities," J. Appl. Phys., 23 (January, 1952), 68-77.
- Reinhart, Edgar A., Robert L. Legan and C. Lin Chun, "Microwave Spectrograph for Linewidth Measurement," Rev. Sci. Instr., 36 (April, 1965), 511-517.
- Sen, S. K., J. Basu and A. K. Ghosal, "Determination of the Dielectric Constant of a Tubular Material at 3 KMHz," J. Appl. Phys., 38 (September, 1964), 601-609.
- Slater, J. C., "Microwave Electronics," Rev. Mod. Phys., 18 (October, 1946), 441-512.
- Spencer, E. G., R. C. LeCraw and L. A. Ault, "Note on Cavity Perturbation Theory," J. Appl. Phys., 28 (January, 1957), 130-132.
- Srivastava, G. P., P. C. Mathur, Krishna and R. M. Mehra, "Dielectric Measurements on Alloy Semiconductors in the Microwave Frequency Region," Indian J. of Pure and Applied Phys., 9 (July, 1971), 453-455.

Tompkins, J. E. and E. G. Spencer, "Retardation Effects Caused by Ferrite Sample Size on the Frequency Shift of Resonant Cavity," J. Appl. Phys., 28 (September, 1957), 969-974.

#### Reports

Bethe, H. A. and J. Schwinger, N.D.R.C. Report DI-117, Cornell University, 1945.